THE ASTROPHYSICAL JOURNAL, 451:308–313, 1995 September 20

DOUBLE CORE EVOLUTION. VIII. THE SPIRAL-IN OF A MAIN-SEQUENCE STAR THROUGH THE ENVELOPE OF AN ASYMPTOTIC GIANT BRANCH COMPANION

HAROLD W. YORKE,[1] PETER BODENHEIMER,[2] AND RONALD E. TAAM[3]
Received 1995 February 13; accepted 1995 March 30

ABSTRACT

A progenitor system for a cataclysmic variable binary consisting of a main-sequence star of 0.7 $M_\odot$ and a 3 $M_\odot$ asymptotic giant branch star (with a carbon-oxygen core of mass 0.7 $M_\odot$) is evolved through the common envelope phase. The two-dimensional axisymmetric simulations show that the entire common envelope is ejected without the two cores merging together. It is demonstrated that the common envelope evolution terminates as a direct result of the spin-up to near corotation of gas in the vicinity of the cores. The evolution of the common envelope has been followed for sufficiently long times to show that the ejected matter remains confined to the equatorial plane at large distances ($\gtrsim 10^{14}$ cm) from the double core. A new feature in the ejected nebula is the appearance of multiple shock fronts which develop as a result of nonuniform energy injection into the envelope. Outward-moving pressure waves form which steepen into shocks as the density falls off in the envelope.

The implications of the results for the origin of cataclysmic variables are discussed.

Subject headings: binaries: close — hydrodynamics — novae, cataclysmic variables — stars: evolution — stars: interiors

1. INTRODUCTION

The properties of the cataclysmic variable binary systems and their immediate progenitor systems (the binary nuclei of planetary nebulae) can be understood if the main-sequence–asymptotic giant branch star progenitor system lost significant mass and angular momentum. This transformation is thought to take place in a common envelope. As described by Paczyński (1976) nearly two decades ago, the origin of cataclysmic variables could be attributed to the gravitational interaction of a main-sequence star with the white dwarf core of its red giant companion with a differentially rotating common envelope. The existence of a new class of systems (planetary nebulae with binary nuclei) was a direct outcome of this scenario, and the first one of its class (UU Sge) was soon found by Bond, Liller, & Mannery (1978). Since that time, many theoretical investigations have been carried out to study the various processes by which mass and angular momentum can be removed from the system. The recent multidimensional hydrodynamics simulations (see Bodenheimer & Taam 1984; de Kool 1987; Livio & Soker 1988; Taam & Bodenheimer 1989, 1991, 1992; Terman, Taam, & Hernquist 1994, 1995; Taam, Bodenheimer, & Rozyczka 1994) have provided important insights into the nature of the mass ejection process and the manner in which the system arrives at its final state. Specifically, the studies show that mass is ejected in all directions, but with the majority of the mass confined to the orbital plane of the system. Futhermore, the phase of severe mass and angular momentum loss from the system ends with the spin-up of the envelope to near corotation once the engulfed companion has encountered the deep envelope layers where a steep density gradient and a flat mass-radius profile exists (Taam & Bodenheimer 1991; Taam et al. 1994). If this characteristic is not present in the structure of the progenitor star, the survival of the remnant binary is not expected, and the system is expected to merge into a single star.

The most recent three-dimensional simulations (Terman et al. 1994, 1995) reveal that gravitational torques lead to rapid decay of the binary orbit until the late stages where spin-up to near corotation leads to a dramatic deceleration of the orbital evolution. This latter phase has also been found in two-dimensional simulations as well (see Taam & Bodenheimer 1991; Taam et al. 1994), since angular momentum lost from the orbital motion is not effectively advected away by material motion from the neighborhood of the orbit region. However, there are no calculations to date which have demonstrated that the entire envelope is ejected. This is, in part, a result of the lack of numerical resolution in the region of the evolved core. Furthermore, the lack of resolution in the outer low-density regions has precluded a detailed examination of the flow structure and density morphology of the nebula surrounding the remnant binary system on length scales significantly greater than the initial binary orbital separation of the progenitor system.

In this paper, we build on our previous studies by considering the evolution of an asymptotic giant branch star with a main-sequence companion. By following the common envelope stage at much higher resolution and over much larger scales than in past studies, we show that systems entering the common envelope phase during the stage of hydrogen and helium shell burning can eject the red giant envelope and survive as a remnant binary provided that steep density gradients exist in the progenitor star. We find that the remnant binary system is characterized by an orbital separation of ~ 15 $R_\odot$ and a period of $\lesssim 6$ days for the parameters studied in this paper.

2. FORMULATION

A common envelope binary consisting of a 0.7 $M_\odot$ main-sequence star and an evolved 3 $M_\odot$ asymptotic giant branch

[1] Astronomisches Institut der Universitaet Wuerzburg, Am Hubland, D-97074 Wuerzburg, Germany; yorke@astro.uni-wuerzburg.de.
[2] University of California Observatories/Lick Observatory, Board of Studies in Astronomy and Astrophysics, University of California, Santa Cruz, CA 95064; peter@lick.ucsc.edu.
[3] Department of Physics and Astronomy, Northwestern University, 2145 Sheridan Road, Evanston, IL 60208; taam@ossenu.astro.nwu.edu.

star with a 0.7 $M_\odot$ carbon-oxygen core is considered. The focus of this study is on the later stages of evolution rather than the initial infall stage. The evolution of the system is started with as large an orbital separation as possible which is consistent with our two-dimensional approximation. We assume the main-sequence star to be situated within a slowly rotating common envelope at an orbital separation of 2×10^{12} cm (about a factor of 20 times smaller than the diameter of the common envelope). The approximation of two-dimensional flow, with averaging over the orbit, is reasonable at this point since the results of Terman et al. (1994) indicate that the timescale for orbital decay is significantly longer than the orbital period at this separation. In addition, the degree of spin-up at this separation is small, since the angular momentum is advected toward the surface by material motion. Our unpublished calculations at an orbital separation of 10^{13} cm, on the other hand, indicate that the two-dimensional approximation is not self-consistent since the orbital decay timescale is comparable to the orbital period. For the case presented here, the two cores revolve many times in their orbit before there is appreciable orbital decay.

As the discussion in § 4 indicates, the orbital decay will not significantly decelerate until the envelope can be spun up to the point where its rotational velocity is a large fraction of the companion's orbital velocity, which can occur only when the orbital separation has decreased within 10^{12} cm for this red giant model. In addition, the ejection of the entire common envelope is not expected until sufficient energy from the orbit has been liberated to account for the envelope's binding energy. Thus, the result of the calculation should be relatively insensitive to our choice of the initial orbital separation taken for the cores.

The hydrodynamical evolution of the common envelope is followed using a modified version of a method developed by Rozyczka (1985). The present work is distinguished from the earlier study of Taam & Bodenheimer (1991) in the treatment of the problem at high numerical resolution afforded by the use of a nested grid approach. This technique involves the use of a number of subgrids of increasingly higher spatial resolution with the dynamical coupling between grids based on the technique of Berger & Oliger (1984) and Berger & Colella (1989) as described in Yorke, Bodenheimer, & Laughlin (1993, 1995) and Ruffert (1993). In this paper we use eight grids in the meridional plane. Each grid is described in cylindrical polar coordinates (r, z) and consists of 60 radial zones and 60 vertical zones with each subgrid chosen to be a factor of 2 smaller in radius. This allows the simulation of the hydrodynamical evolution over length scales to 1.7×10^{14} cm. The smallest zone in the innermost grid corresponds to about 2.3×10^{10} cm. In contrast to previous two-dimensional simulations, the white dwarf core of the asymptotic giant branch star is not fixed in position, but allowed to move in its orbit as well. In this work, the two cores are averaged in angle over the orbit and are treated as a single ring. They interact with the envelope only through gravitational effects, which are approximated by a softened ring potential. The choice of an identical mass for the white dwarf core as the main-sequence companion allows us to describe the two cores in this way. In this formulation of the problem, there is no inner boundary radius for the red giant. Hence, the only boundary condition is applied at the outer edge. During the early part of the evolution, when the outer part of the red giant is still hydrostatic, an artificial pressure is introduced in the external medium to prevent spurious envelope expansion. This procedure is necessary because the outer part of the atmosphere is not spatially resolved. The external pressure is gradually reduced as the hydrodynamic flow approaches the surface of the red giant. Through a series of numerical tests, the pressure-reduction formula was adjusted so that it did not result in spurious mass loss. Once the flow approaches the edge of the grid at 2×10^{14} cm, a transmitting boundary condition is applied there, which involves setting the gradients of pressure, temperature, and velocity equal to zero.

The loss of energy and angular momentum from the two cores is treated similarly as in Taam & Bodenheimer (1991) as modified by the results of Taam et al. (1994). Specifically, the energy dissipation rate per unit volume, ϵ, and the torque per unit volume, j are given as

$$\epsilon = \frac{f\rho V_{\rm rel}^3}{2\pi r} \tag{1}$$

and

$$j = \frac{f\rho V_{\rm rel}^2}{2\pi}, \tag{2}$$

where ρ, $V_{\rm rel}$, and r are the local density, relative velocity of each core with respect to the local gas, and the distance from the common center of mass, respectively. The factor f is a function of the Mach number of the flow and has been taken from the work of Shima et al. (1985). The total dissipation rate and angular momentum loss rate is obtained by the volume integral over the Bondi-Hoyle accretion radius of each core. Taam et al. (1994) show that the rates so obtained are about equivalent to those generated by gravitational torques in a nonaxisymmetric simulation.

For the description of the orbital evolution, it is assumed that the mass of the two cores remains constant. This is a very good approximation, since the results of Hjellming & Taam (1991) indicate that the amount of mass accreted during the entire evolution is small ($\lesssim 0.01\ M_\odot$). In addition, there is little mass between the two cores in the later phases of the double core evolution, since there is $\lesssim 0.03\ M_\odot$ within a radius of 10^{12} cm in the initial model. At $t = 11$ yr the mass within 10^{12} cm has dropped to about $0.0001\ M_\odot$.

3. NUMERICAL RESULTS

The initial common envelope model was constructed from a one-dimensional red giant model on which is superposed the gravitational potential of an annulus with $1.4\ M_\odot$ and a radius of 10^{12} cm. The model was relaxed using a damping technique. After about 1.5 yr of evolution time, which is about 36 times the orbital period of the two cores, the model had reached a state of mechanical equilibrium. At this point the double core system was allowed to evolve with the energy and angular momentum lost from the orbital motion deposited in the common envelope. The orbital evolution is illustrated in Figure 1, where it can be seen that the orbital separation decreases rapidly from 2×10^{12} cm to 1.3×10^{12} cm within 0.83 yr after the initial relaxation phase. Thereafter, the orbital evolution decelerates with the orbital decay timescale increasing to greater than 300 yr after an additional evolution time of 8.6 yr. A final orbital separation for the two cores was reached at 10^{12} cm by the end of the calculation.

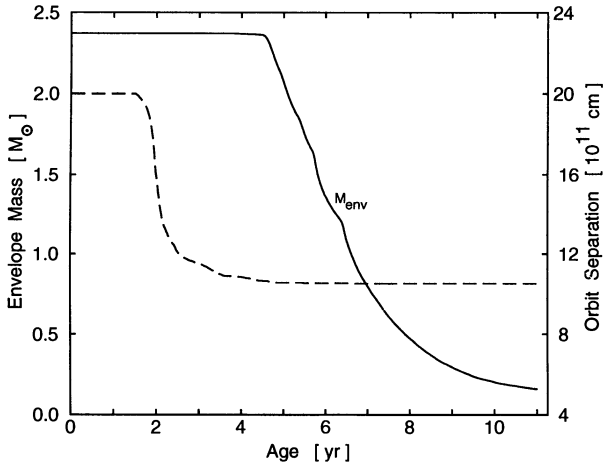

FIG. 1.—Variation of the orbital separation between the two cores (*dashed line*) and the mass of the common envelope (*solid line*) as a function of time. The envelope mass is defined as the amount of mass within the computational grid.

The rate at which energy is deposited into the common envelope is illustrated in Figure 2. It is found that the rate rises gradually until it peaks at $\sim 10^{39}$ ergs s^{-1}, at a time when the orbital separation had decreased from 2×10^{12} cm to 1.5×10^{12} cm. Subsequently, the energy deposition rate declined to 10^{36} ergs s^{-1} at an age of 6 yr and then decreased slowly to $\sim 10^{35}$ ergs s^{-1} after a total evolution time of 10 yr. The gradual decline to this low level reflected the reduction in the density and the spin-up to near corotation (to within 20%) of gas in the vicinity of the two cores. This spin-up follows from the reduction in energy deposition rate associated with the loss of mass from the common envelope. As a result of the expansion of the common envelope, the density of matter and, consequently, the energy deposition rate decreased. This trend was further accentuated by the reduction in the relative velocity of the common envelope relative to the two cores. This follows from the fact that matter in the vicinity of the double core is no longer accelerated to velocities greater than the velocity of escape. Consequently, the matter does not advect angular momentum away from the orbit over large distances as in earlier phases of the evolution, and the lost orbital angular momentum is transformed into the spin of the gas in the region neighboring the two cores. This leads to a further reduction of the energy input rate into the common envelope, to a much slower energy loss from the orbit, and to a significant deceleration of the orbital evolution.

As a result of the energy injection into the common envelope, significant mass is lost. The amount of mass remaining in the outermost computational grid is illustrated as a function of evolution time in Figure 1. It can be seen that the mass in the common envelope begins to decrease rapidly about 3 yr after the initial relaxation process. The time delay is a consequence of our definition of mass loss: i.e., only material leaving the outermost grid ($r_{max} = z_{max} = 1.7 \times 10^{14}$ cm) is considered "lost." The phase of mass loss occurred immediately after the peak of the energy deposition rate was reached. It can be seen that the mass-loss rate was constant at about 0.63 $M_\odot$ yr^{-1} for 2.4 yr, and then it tapered off gradually. By the end of the calculation 2.1 $M_\odot$ had been lost from the common envelope. Much of the remaining 0.2 $M_\odot$ is still expanding at greater than the escape velocity. In fact, we find that only a maximum of 0.02 $M_\odot$ is still bound. Because of numerical difficulties in determining the overall energy balance (associated with the large external volume into which the gas expands and within which the pressure initially was set artificially high), an accurate value for the efficiency of the mass ejection process, defined as the ratio of the initial binding energy of the envelope to the energy lost from the orbit, cannot be obtained. We estimate that the resulting efficiency is similar to that obtained in previous papers (Taam & Bodenheimer 1989), about 30%–60%.

The velocity field and the density distribution in the common envelope for two evolutionary times are shown in Figures 3–4. The highest velocities are present in the vicinity of the double core, and this region propagates outward as a function of time. The fact that the mass ejection originates in the deep interior and not at the surface provides evidence that the treatment of the outer atmosphere does not influence the

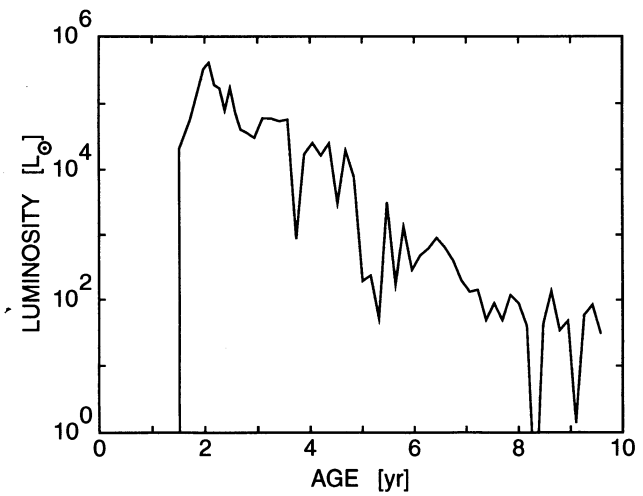

FIG. 2.—Time variation of the energy deposition rate into the common envelope by the two cores. For the initial period of relaxation into a state of mechanical equilibrium, no energy was deposited.

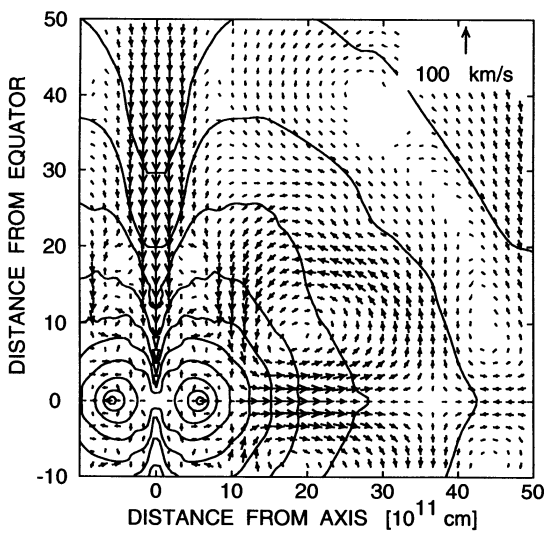

FIG. 3.—Distribution of gas and velocity field deep within the common envelope after an evolution time of 2.8 yr. Velocity scale is indicated at the upper right. Isodensity contours range from $\log \rho = -6.2$ to -4.4 ($\Delta \log \rho = 0.2$).

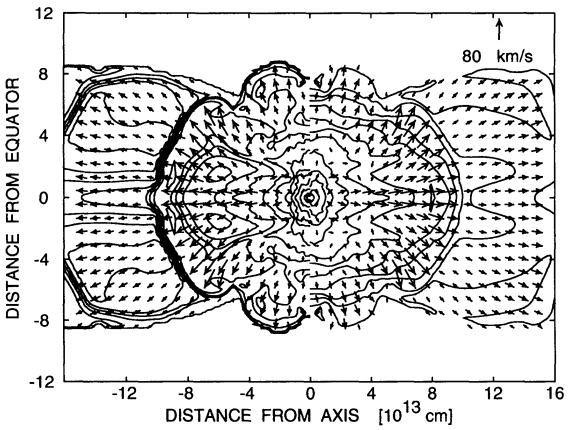

FIG. 4.—Distributions of density, temperature, and velocity field within the common envelope after an evolution time of 4.21 yr. Velocity scale is indicated at the upper right. Isodensity contours are plotted to the right of the rotation axis; isotemperature contours are illustrated to the left. The contour intervals range from $\log \rho = -11.5$ to -6.0 for the density ($\Delta \log \rho = 0.5$) and from $\log T = 2.6$–5.4 for the temperature ($\Delta \log T = 0.2$). Note the formation of multiple shock structures in the temperature distribution.

results on a qualitative level. Although some mass has been lost in the polar direction ($\lesssim 10\%$), it is significant that the envelope is flattened in the equatorial direction. In fact, it is seen that the mass is confined to the orbital plane to distances as great as 1.7×10^{14} cm. In addition, there is evidence for shock structures in the common envelope which are most easily discerned in the temperature distribution (see Fig. 4). Because the energy injection is not smooth (primarily as a result of variations in the relative velocity) but semioscillatory, outward moving pressure waves are produced close to the center. These acoustical waves steepen into shocks due to the density falloff in the expanding envelope. These structures eventually died out for late evolutionary stages because the energy injection became less significant.

4. DISCUSSION

The multidimensional hydrodynamical evolution of the common envelope stage has been followed in the meridional plane of a binary system consisting of a 3 $M_\odot$ asymptotic giant branch star (with a 0.7 $M_\odot$ white dwarf core) and a 0.7 $M_\odot$ main-sequence star. It is found that for this asymptotic giant branch star the entire common envelope can be ejected without the two cores merging together. This ejection is accomplished as a result of expansion assisted by the centrifugal effects associated with the transfer of orbital angular momentum into spin angular momentum of the common envelope and by the dissipation of orbital energy into thermal energy within the gravitational interaction region.

In contrast to previous two-dimensional studies, the ejection of mass has been followed over a much larger region extending out to about 10 times the initial stellar radius of the asymptotic giant branch star. It is found that the mass distribution remains confined toward the orbital plane, confirming results obtained from calculations in which a more limited region was modeled. The ejected mass tends to form a dense flattened and expanding structure surrounding the double core system. The further evolution to longer timescales is expected to lead to the ejection of the remaining mass in the polar direction and to the formation of a toroidal-like structure. The formation of this structure is a natural consequence of the asymmetry in the problem and provides a mechanism to produce a density contrast between the polar and equatorial directions. The interaction of a fast stellar wind emitted from the remnant core of the asymptotic giant branch star (as it evolves to higher effective temperature) with this structure may be responsible for the variety of aspherical planetary nebula shapes observed (Frank et al. 1993; see also Kwok 1982 and Kahn 1982). We note that the calculations presented in this study indicate that the mass ejection process is not smooth, and that it exhibits transitory phases accompanying the formation of shock structures.

We find that the system reaches a final orbital separation of 15 $R_\odot$ corresponding to an orbital period of 5.74 days. Because nearly all the mass of the common envelope has been ejected, it is not likely that the final orbital parameters of the remnant system will depart significantly from that found in the calculation. As emphasized by Taam & Bodenheimer (1991), the existence of a steep density gradient exterior to the hydrogen- and helium-burning shells of the progenitor star is essential for decelerating the orbital evolution to terminate the common envelope phase. This requirement is necessary in order that the gas in the vicinity of the two cores is spun up to near corotation. As a result, the ejection of matter becomes less effective because the wind mass loss drops as the density of the outflowing matter declines. In addition, the matter interior to the orbit will contract to the white dwarf core as the timescale for orbital decay increases and approaches the thermal timescale of these layers. The contraction reflects the stellar readjustment associated with the tendency for maintenance of the energy production in the nuclear burning shells (see Taam & Bodenheimer 1991) at the same level as in earlier phases in response to the reduction of mass in its overlying layers.

Provided that sufficient orbital energy is released from the two cores to unbind the common envelope, the structure of the progenitor star determines whether the main-sequence companion will merge with the white dwarf core or will survive intact as a remnant binary. As indicated above, the existence of a sharp density gradient and a flat mass-radius profile is important for slowing the orbital evolution of the two cores to the extent that the mass layers interior to the orbit can contract onto the white dwarf core. For a flat mass-radius profile, the region of gravitational interaction of the two cores involves little mass, and the rate of energy loss from the orbit via dissipation or gravitational spin-up is low. To illustrate this type of structure, we present the density distribution and mass distribution of a 5 $M_\odot$ red giant branch star in two different evolutionary phases in Figures 5 and 6, respectively. In the less evolved case, the degenerate carbon-oxygen core is beginning to form, whereas in the more evolved case the star is characterized by a 0.8 $M_\odot$ degenerate carbon-oxygen core with an overlying helium layer of 0.12 $M_\odot$. It can be seen that the red giant in a more evolved phase exhibits a sharper density gradient above the nuclear burning shell near 1 $M_\odot$ than the less evolved giant. Specifically, the density varies sharply over 5 orders of magnitude and 9 orders of magnitude above the nuclear burning shells in these two cases. Furthermore, the mass-radius profile is flatter and extends to larger radii for the more evolved case. In particular, it is seen that the flat profile extends to radii $\sim 10^{12}$ cm in the more evolved model. This type of profile indicates that once the companion star encounters this region, say 5×10^{11} cm, there is little mass contained in its gravitational interaction region which extends both interior and exterior to this radius. We note that the amount of mass contained in the gravitational interaction region is less

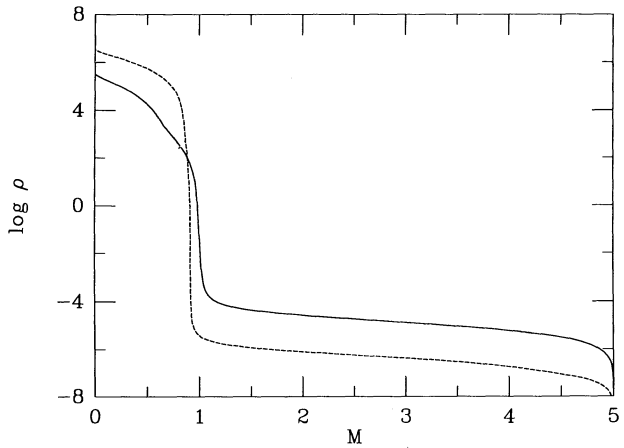

FIG. 5.—Density distribution with respect to mass (in units of $M_\odot$) for a 5 $M_\odot$ red giant star in two different evolutionary phases. Note that the density gradient is much steeper in the more evolved model (*dashed line*) with respect to the less evolved model (*solid line*).

than inferred from Figure 6, since this figure illustrates the mass contained within a spherical region whereas the gravitational interaction region is better described as an annulus. Hence, the timescale of the orbital evolution must increase rapidly. On the other hand, for the case of the less evolved model, this does not occur until an orbital separation of $\sim 10^{11}$ cm is reached. The ejection of the envelope and the formation of a precataclysmic variable (i.e., a detached system consisting of a pre–white dwarf star and a main-sequence star) is favored in the case of a more evolved configuration and of a more massive main-sequence companion for an asymptotic giant branch star of a given mass. This follows from the fact that the initial binding energy of the common envelope is lower for more evolved stars and the energy released from the binary orbit is greater for more massive companions. In contrast, if there is insufficient energy to eject the envelope or if the structure of the region overlying the nuclear burning shells of the progenitor star is not characterized by a flat mass-radius profile, the system is likely to merge.

Further constraints on the survival of the binary as a precataclysmic variable can be imposed on the progenitor system parameters by the requirement that the remnant binary system is detached. That is, the secondary star must reside within its Roche lobe after the common envelope has been ejected. This implies that after the main-sequence secondary has relaxed into a state of thermal equilibrium, it is smaller in size than its corresponding Roche lobe. Thus, the condition

$$R < \frac{0.49q^{2/3}}{0.6q^{2/3} + \ln(1 + q^{1/3})} A \qquad (3)$$

must be satisfied, where we have taken the Roche lobe relation from Eggleton (1983). Here A is the orbital separation and q is the mass ratio of the detached system, M_s/M_p, with M_s and M_p denoting the mass of the main-sequence secondary and the white dwarf primary, respectively. For application to precataclysmic variables, $M_s < M_p$. For white dwarfs less massive than 1.4 $M_\odot$ and main-sequence companions less massive than 1 $M_\odot$, the orbital separations exceeding $\sim 2.6\ R_\odot$ ensure that this condition is satisfied. The relation between the mass of the progenitor star and the mass of the core such that the mass-radius profile is flat for orbital separations $\gtrsim 2.6\ R_\odot$ is shown in Figure 7. It is seen that the relation is monotonic and that the mass of the white dwarf core remnant increases with the mass of the progenitor asymptotic giant branch star. We note that this mass relation provides an actual lower limit to the white dwarf mass for a given progenitor star, since an evolved giant with a more massive white dwarf will have flat mass-radius profile extending beyond 2.6 $R_\odot$ leading to a deceleration of the orbital evolution at a larger orbital separation and longer orbital period. Above the solid line in Figure 7, a remnant binary will survive provided that sufficient energy is available to eject the common envelope. On the other hand, below the curve it is likely that a merger takes place, since the orbital evolution is not sufficiently decelerated. From the conceptual framework outlined above, one can conclude that the efficiency of the mass ejection process is not likely to be constant but will vary from system to system depending, in part, on the location for which the mass-radius profile in the common envelope is sufficiently flat.

A determination of the progenitor systems for the cataclysmic variables requires the knowledge of the history of the star formation rate, the initial distribution of the primary and secondary masses and orbital separations of the initial main-

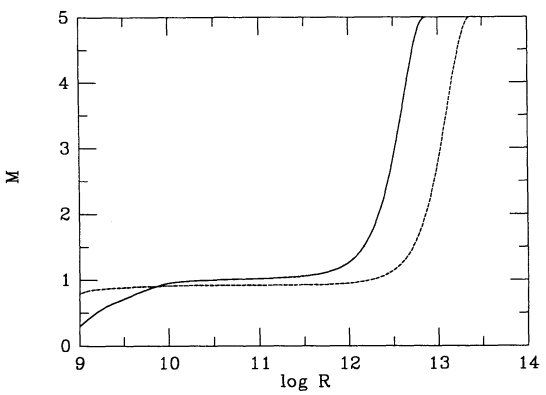

FIG. 6.—Mass-radius profile for a 5 $M_\odot$ red giant star in two different evolutionary phases. Mass is expressed in $M_\odot$. The more evolved model with a larger stellar radius (*dashed curve*) exhibits a flatter profile to larger radii than the less evolved model (*solid curve*).

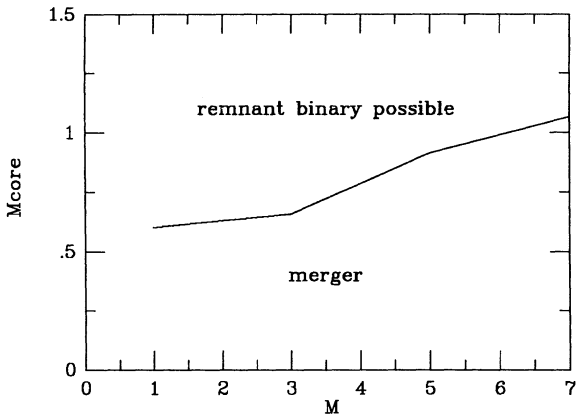

FIG. 7.—Core mass–progenitor mass relation for which the mass-radius profile is flat to a radius of 2.6 $R_\odot$. Above the curve, the mass-radius profile extends beyond 2.6 $R_\odot$ and below this curve, the mass-radius profile either is not flat or does not extend to 2.6 $R_\odot$. Core mass and progenitor mass are in units of $M_\odot$.

sequence binaries (see Ritter et al. 1991; de Kool 1992; Han, Podsiadlowski, & Eggleton 1995), and the efficiency of the mass ejection process in the common envelope phase of evolution. As emphasized in this study, the constraints imposed on the system parameters by the likelihood that the system can avoid merger is equally important as well. The inclusion of this additional constraint should be included in future population synthesis studies. An investigation of the ramifications of these important inputs to the population synthesis studies will be the subject of future investigations.

This research has been supported by NSF grants AST-9113150 and AST-9415423. H. W. Y. acknowledges travel support by the DFG.

REFERENCES

Berger, M. J., & Colella, P. 1989, J. Comput. Phys., 82, 64
Berger, M. J., & Oliger, J. 1984, J. Comput. Phys., 53, 484
Bodenheimer, P., & Taam, R. E. 1984, ApJ, 280, 771
Bond, H. E., Liller, W., & Mannery, E. J. 1978, ApJ, 223, 252
de Kool, M. 1987, Ph.D. thesis, Univ. Amsterdam
———. 1992, A&A, 261, 188
Eggleton, P. P. 1983, ApJ, 268, 368
Frank, A., Balick, B., Icke, V., & Mellema, G. 1993, ApJ, 404, L25
Han, Z., Podsiadlowski, P., & Eggleton, P. P. 1995, MNRAS, 272, 800
Hjellming, M. S., & Taam, R. E. 1991, ApJ, 370, 709
Kahn, F. D. 1982, in Planetary Nebula, ed. D. R. Flower (Dordrecht: Reidel), 305
Kwok, S. 1982, ApJ, 258, 280
Livio, M., & Soker, N. 1988, ApJ, 329, 764
Paczyński, B. 1976, in IAU Symp. 73, The Structure and Evolution of Close Binary Systems, ed. P. Eggleton, S. Mitton, & J. Whelan (Dordrecht: Reidel), 75
Ritter, H., Politano, M., Livio, M., & Webbink, R. F. 1991, ApJ, 376, 177
Rozyczka, M. 1985, A&A, 143, 59
Ruffert, M. 1993, A&A, 280, 141
Shima, E., Matsuda, T., Takeda, H., & Sawada, K. 1985, MNRAS, 217, 367
Taam, R. E., & Bodenheimer, P. 1989, ApJ, 337, 849
———. 1991, ApJ, 373, 246
———. 1992, in X-Ray Binaries and Recycled Pulsars, ed. E. P. J. van den Heuvel & S. A. Rappaport (Dordrecht: Kluwer), 281
Taam, R. E., Bodenheimer, P., & Rozyczka, M. 1994, ApJ, 431, 247
Terman, J. L., Taam, R. E., & Hernquist, L. 1994, ApJ, 422, 729
———. 1995, ApJ, 445, 367
Yorke, H. W., Bodenheimer, P., & Laughlin, G. 1993, ApJ, 411, 274
———. 1995, ApJ, 443, 199